Published in final edited form as:
Clin Cancer Res. 2013 January 1; 19(1): 128–137. doi:10.1158/1078-0432.CCR-12-2654.

Targeted Delivery of Paclitaxel to EphA2-Expressing Cancer Cells

Si Wang[1,#], **Roberta Noberini**[1,#], **John L. Stebbins**[1,#], **Swadesh Das**[2], **Ziming Zhang**[1], **Bainan Wu**[1], **Sayantan Mitra**[1], **Sandrine Billet**[3], **Ana Fernandez**[3], **Neil A. Bhowmick**[3], **Shinichi Kitada**[1], **Elena B. Pasquale**[1], **Paul B. Fisher**[2], and **Maurizio Pellecchia**[1,*]

[1]Cancer Research Center, Sanford-Burnham Medical Research Institute, 10901 N. Torrey Pines Rd., La Jolla, CA 92037, USA

[2]Departments of Human & Molecular Genetics, Virginia Commonwealth University, School of Medicine, 1101 East Marshall Street, Sanger Hall Building, Room 11-015, Richmond, VA 23298-0033, USA

[3]Department of Medicine, Cedars-Sinai Medical Center, 8750 Beverly Blvd, Los Angeles, CA 90048, USA

Abstract

Purpose—YSA is an EphA2-targeting peptide that effectively delivers anti-cancer agents to prostate cancer tumors (1). Here, we report on how we increased the drug-like properties of this delivery system.

Experimental Design—By introducing non-natural amino acids, we have designed two new EphA2 targeting peptides: YNH, where norleucine and homoserine replace the two methionine residues of YSA, and dYNH, where a D-tyrosine replaces the L-tyrosine at the first position of the YNH peptide. We describe the details of the synthesis of YNH and dYNH paclitaxel conjugates (YNH-PTX and dYNH-PTX) and their characterization in cells and *in vivo*.

Results—dYNH-PTX showed improved stability in mouse serum and significantly reduced tumor size in a prostate cancer xenograft model and also reduced tumor vasculature in a syngeneic orthotopic allograft mouse model of renal cancer compared to vehicle or paclitaxel treatments.

Conclusion—This study reveals that targeting EphA2 with dYNH drug conjugates could represent an effective way to deliver anti-cancer agents to a variety of tumor types.

Translational Relevance—Overexpression of the EphA2 positively correlates with tumor malignancy and poor prognosis. For this reason, EphA2 is an attractive target for cancer cell specific drug delivery. In this study, we report on the development of dYNH, an EphA2 targeting peptide that when coupled to paclitaxel (PTX) has favorable pharmacological properties and possesses powerful anti-tumor activity *in vivo*. dYNH-PTX may allow for an expanded

[*]To whom correspondence should be addressed. mpellecchia@sanfordburnham.org.
[#]S. W., R.N. and J.L.S. contributed equally to this work.

Author Contributions

S.W., R.N. and J.L.S. contributed equally to this work. M.P. designed the research strategy for the peptide conjugates. S.W. synthesized and purified the peptide-PTX conjugates. R.N. performed the ELISA and cell culture experiments. J.L.S. and S.K. performed the tumor xenograft experiments in Figure 6A and S1, while S.D. performed the experiment reported in Figure 6B. Z.Z and B.W performed expression and purification of the EphA2 LBD and the subsequent NMR and ITC experiments. P.B.F. helped design and analysis of the tumor xenografts with PC3M cells, in Figure 6B. E.B.P. supervised the experiments reported in Figures 4 and 5. S.B. and A.F. performed the *in vivo* renal cancer allograft studies under the supervision and direction of N.A.B. J.L.S. and M.P. wrote the manuscript with help from the other authors.

therapeutic index of paclitaxel as well as precluding the need for complex formulations and long infusion times.

INTRODUCTION

Chemotherapeutic agents, such as the mitotic inhibitor paclitaxel, are nonselective (2) and thus often cause many adverse side effects such as systemic toxicity. A potential solution to this difficult problem is to take advantage of the growing number of tumor specific cell surface biomarkers to design targeted delivery modules (3, 4). Utilization of these targets has resulted in a wide variety of tumor-homing motifs coupled to a variety of anticancer and imaging agents (3-8). Humanized monoclonal antibodies are currently the most advanced homing agents, and take advantage of the selective nature of antibody-antigen interaction to target and bind with high affinity to validated cancer cell antigens. Despite the advantages, there are clinical limitations to the use of antibodies. These include protein stability and formulation issues, the risk of an adverse immune response, and high manufacturing costs (9, 10).

Short peptides that target tumor-specific markers also show promise for selective tumor targeting. Tumor specific peptide sequences able to bind cancer cell-specific motifs have been identified using combinatorial chemistry methods and phage display techniques (11-23). For example, peptides such as iRGD and RC-160 have been used to target neuropilin-1 (5) and the somatostatin receptor (3), respectively. Peptides can be conjugated to anti-cancer agents in various drug/peptide ratios. Furthermore, some tumor targeting peptides are able to not only target tumor cells but also facilitate cell penetration of both the peptide and the payload (24). The ability to identify tumor cells as well as mediate drug internalization can result in an increase in drug activity and a reduction in drug toxicity, thus making homing peptides attractive drug delivery vehicles.

The Eph receptors are a family of receptor tyrosine kinases that play a role in neuronal connectivity, blood vessel development and numerous other physiological processes by influencing cell shape and migration through their effects on the actin cytoskeleton as well as cell survival and proliferation (25-27). They are also involved in numerous pathological processes, including cancer (26). In tumor tissue, the Eph receptors modulate cell-cell communication involving not only tumor cells but also tumor stroma and vasculature (28, 29), thus differentiating them from traditional oncogenes that function only in tumor cells. Specifically, the family member EphA2 is overexpressed in many types of cancers (1, 26, 27, 30-32), where its presence has been linked to tumor malignancy and poor prognosis (26, 32). In addition, EphA2 is expressed in the tumor vasculature and promotes tumor angiogenesis (33), making it a compelling target to reduce angiogenesis at the tumor site. Thus, due to its association with a wide variety of cancers and its multifaceted role in cancer progression, EphA2 is an attractive target for drug design (25).

YSA (amino acid sequence YSAYPDSVPMMS) is a peptide identified by phage display that selectively targets EphA2 and, similarly to the natural EphA2 ligand ephrin-A1, causes receptor activation and internalization (17, 34). A version of this peptide coupled to magnetic nanoparticles was used to capture circulating ovarian cancer cells *in vivo* (35) and YSA-functionalized nanogels were used to chemosensitize cancer cells expressing EphA2 by mediating siRNA delivery and internalization (36, 37). We recently reported that when YSA is conjugated to paclitaxel, it targets EphA2 over-expressing prostate cancer cells *in vivo*, inhibiting tumor growth in a prostate cancer xenograft model more effectively than paclitaxel alone (1). Here we describe our efforts to improve the pharmacological properties and efficacy of YSA-drug conjugates by introducing non-natural amino acids in the targeting motif.

RESULTS

Design and Synthesis of YNH-Paclitaxel (YNH-PTX) and dYNH-Paclitaxel (dYNH-PTX)

Previously we successfully used the YSA-paclitaxel (YSA-PTX) conjugate to target prostate cancer cells *in vivo* (1). However, the two methionine residues in the YSA peptide are susceptible to oxidation *in vivo* and thus represent a likely liability. We therefore replaced the two methionines with unnatural amino acids to generate the YNH peptide (YSAYPDSVP(L-norleucine)(L-homoserine)S). With the aim of further improving the stability of the peptide, we also replaced the L-tyrosine at the N-terminus of the YNH peptide with a D-tyrosine to generate the dYNH peptide (ySAYPDSVP(L-norleucine)(L-homoserine)S) (Figure 1). The subsequent synthesis of the YNH-PTX and dYNH-PTX conjugates was based on our recently reported selective protection/deprotection strategy and click chemistry (Figure 1) (1). The integrity and purity of the final peptide-drug conjugates was confirmed by HPLC, 1D and 2D NMR and mass spectrometry (see Supplemental Material).

Characterization of YNH-PTX and dYNH-PTX

We initially employed ^{15}N-labeled EphA2 ligand binding domain (residues 27-200) and 2D [^{1}H-^{15}N] HSQC spectra to monitor protein-peptide interactions. Chemical shift perturbations in 2D [^{1}H-^{15}N] HSQCs, indicative of peptide interactions with residues in the EphA2 ligand-binding domain, were clearly observed in the presence of YNH-PTX or dYNH-PTX, but not with the scrambled control peptide conjugate, DYP-PTX (Figures 1 and 2). Quantitative isothermal titration calorimetry (ITC) analysis further confirmed that YSA-PTX, YNH-PTX and dYNH-PTX bind to the isolated recombinant ligand-binding domain of EphA2 with apparent K_d values of 9.8 μM, 2.2 μM, and 33 μM, respectively, whereas the control DYP-PTX failed to appreciably bind under the same experimental conditions (Figure 3). We further confirmed the relative affinities of the PTX-coupled peptides for EphA2 using an ELISA measuring EphA2 Fc binding to the biotinylated peptides immobilized onto ELISA wells. Using this method, relative affinity values of 0.17 and 3.7 were obtained from the comparison of YNH-PTX and dYNH-PTX, respectively, with YSA-PTX. The control DYP-PTX again failed to bind under the same experimental conditions (Figure 4A).

The relative stability of YSA-PTX, YNH-PTX, and dYNH-PTX is an important, but difficult characteristic to assess. The molecules are not amenable to standard LC/MS detection because of an inherent inability to ionize. Nonetheless, we were able to determine the relative stability of YSA-PTX, YNH-PTX, and dYNH-PTX in PC3 cell cultures and in mouse serum by assaying the ability of each peptide conjugate to compete with ephrin-A5 for EphA2 binding following incubation with cultured PC3 cells or in serum. This approach has the advantage to determine more directly the amount of active (i.e. EphA2-binding) peptide. As predicted, dYNH-PTX is the most stable with about 49% and 68% activity remaining after 24 h incubation in culture medium or serum respectively, followed by YNH-PTX (29% or 13% remaining at 24 h) and YSA-PTX (0% remaining at 24 h) (Figure 4B).

YNH-PTX and dYNH-PTX target selectively EphA2 over-expressing tumor cells

To investigate EphA2 targeting and selectivity, we visualized YNH-PTX and dYNH-PTX internalization in EphA2 over-expressing PC-3M-luc-C6 (PC3M) cells and in LNCaP cells, which do not express EphA2 (1). Incubation of the C-terminally biotinylated peptides coupled to streptavidin-conjugated red fluorescent quantum dots (Qdots) with the two cell types showed that YNH-PTX and dYNH-PTX were internalized only in the EphA2 positive PC3M cells, but not in LNCaP cells (Figure 5A). The fluorescence from the Qdots overlaps with staining for EphA2 and the lysosomal marker Lamp1 in PC3M cells, suggesting that

YNH-PTX and dYNH-PTX mediate cellular uptake of EphA2 and the Qdots into lysosomes (Figure 5A). Moreover, we confirmed that even when not coupled to Qdots, YNH-PTX and dYNH-PTX cause EphA2 internalization into PC3M cells and receptor co-localization with the lysosomal marker, similar to the ephrin-A1 Fc ligand (Figure 5B). On the contrary, the DYP-PTX scramble peptide is not internalized into PC3M cells and also fails to trigger EphA2 internalization (Figure 5A,B). YNH-PTX and dYNH-PTX, but not DYP-PTX, also cause EphA2 tyrosine phosphorylation, which is indicative of receptor activation, and concomitant loss of the receptor from the surface of PC3M cancer cells (Figure 5C). These data indicate that the YNH-PTX and dYNH-PTX conjugates can mediate effective EphA2 internalization of PTX into cells, suggesting that they could be useful for targeting cancer cells expressing this receptor.

dYNH-PTX targets tumors in vivo

The combination of the ability of dYNH-PTX to induce EphA2 activation and internalization and its improved stability in mouse serum warranted further evaluation *in vivo*. Therefore, we tested the effect of dYNH-PTX in PC3M tumor xenografts. Tumor-bearing mice were treated three times weekly with an intravenous injection of PTX, dYNH-PTX or vehicle control for three weeks. Significant tumor growth inhibition ($p < 0.05$) was observed with dYNH-PTX as compared to an equimolar dose of PTX (Figure 6A). Moreover, mouse body weights were not affected by dYNH-PTX administration in comparison to administration of vehicle control (not shown), and blood chemistry analysis revealed no adverse signs of toxicity in the dYNH-PTX-treated mice (Supplementary Table 1). In a separate repeated experiment, we also compared control vehicle and PTX groups with groups treated with dYNH-PTX, YSA-PTX, or DYP-PTX (Figure 6B). In this experiment, tumors in the dYNH-PTX-treated group become undetectable after 14 days of treatment. The observed tumor regression in the dYNH-PTX-treated group (Figure 6B) is in agreement with the results reported in Figure 6A, where 2 out 5 mice treated with dYNH also experienced tumor shrinkage. Moreover, the scrambled peptide-PTX conjugate (DYP-PTX) was ineffective *in vivo* (Figure 6B). This latter observation was further confirmed in a separate xenograft study (Supplementary Figure S1).

dYNH-PTX decreases tumor vascularization in a mouse renal tumor model

Recent studies have shown that overexpression of EphA2 in renal cell carcinoma correlates with poorer prognosis and increased vascularization (38). Thus, we tested the efficacy of dYNH-PTX using an orthotopic renal cancer model where EphA2 expressing RENCA renal cancer cells were grafted in the renal capsule of syngeneic BalbC mice and grown for four weeks. The mice were treated with vehicle, PTX, or dYNH-PTX only for the final week prior to harvesting the tumors. There was no significant difference in tumor growth inhibition between the groups treated with dYNH-PTX as compared to the group treated with an equimolar dose of PTX (Figure 6C). However, both treatments significantly decreased tumor volume compared to the vehicle control ($p < 0.003$). Strikingly, the three dYNH-PTX treatments in the fourth week after tumor grafting caused a significant decrease in tumor vasculature, as determined by CD31 staining, compared to vehicle or PTX alone ($p = 0.001$ by ANOVA) (Figure 6D). dYNH-PTX did not, however, affect the vasculature of the normal host kidney parenchyma (data not shown). Of note is that while RENCA cells do express EphA2, the levels of EphA2 do not seem to be as high as in the PC3 cells (Supplementary Figure S2), perhaps explaining why dYNH-PTX was not as efficacious as in the PC3 xenograft in promoting tumor regression.

DISCUSSION

The benefit of chemotherapy is often mitigated by negative side effects linked to a lack of selectivity (2). As a result, recent cancer research has been focused on exploiting tumor specific, cell-penetrating molecules as vehicles for selective anti-cancer drug delivery. Here we describe the next generation of EphA2-targeting peptide-drug conjugates: YNH-PTX and dYNH-PTX. Both YNH-PTX and dYNH-PTX effectively target EphA2 and are able to induce receptor activation, internalization and delivery to lysosomes, which likely causes the release of PTX inside the cancer cells. Our previous work established that a YSA-PTX conjugate affords a significant increase in the amount of drug delivered to tumors as compared with administration of free paclitaxel (1). In this study, we show that dYNH-PTX inhibits the growth of EphA2-expressing tumors more effectively than PTX, and even causes the disappearance of some tumors, suggesting that the improved stability of dYNH-PTX compensates for its decrease in affinity. In addition, consistent with EphA2 expression in tumor blood vessels (29), treatment with dYNH-PTX affected the tumor vasculature in an immune competent model of late stage renal cancer progression, suggesting that this peptide could target not only the tumor cells but also the tumor vasculature. However, the specific mechanism underlying the vascular changes remains to be elucidated.

Exploiting EphA2 as a cancer specific target is attractive due to the fact that EphA2 expression is limited in normal tissues (26, 27, 30, 32). In addition, in normal epithelial cells EphA2 is presumably bound to endogenous ephrin ligands and, as a result, it likely cannot be effectively targeted, whereas in EphA2 over-expressing tumors the receptor is not frequently co-expressed with ephrin ligands (39-42). Therefore, using EphA2-targeting peptides for drug delivery may reduce exposure of normal tissues to cytotoxic drugs, presumably reducing toxic side effects.

The anti-cancer activity of the EphA2-targeting peptide-drug conjugates can be attributed to tumor tissue penetration and selectivity. Paclitaxel is actively transported into cells rather than relying on passive transport, which is the case when a tumor selective molecule lacks the ability to facilitate internalization. In addition, dYNH-PTX affected the tumor-associated vasculature in an immune competent model of late stage renal cancer progression. As a result, dYNH-PTX may expand the therapeutic index of paclitaxel to a point where increased quantities could be safely used. dYNH conjugation may also increase water solubility, making paclitaxel more easily delivered (43) without the use of complex formulations and long infusions.

In summary, by optimizing the sequence of the YSA peptide, we have identified the YNH and dYNH peptides as the next generation of EphA2-targeting peptides. In particular, we have shown that dYNH-PTX has more favorable properties and possesses a powerful anti-tumor activity *in vivo*. Future optimization studies will focus on increasing the affinity of dYNH-PTX for EphA2 without compromising its stability in order to obtain an even more powerful targeting agent.

EXPERIMENTAL PROCEDURES

Chemical synthesis and purification

– Unless otherwise noted, all reagents and anhydrous solvents were obtained from commercial sources and used without purification. All reactions were performed in oven-dried glassware. All reactions involving air or moisture sensitive reagents were performed under a nitrogen atmosphere. Silica gel chromatography was performed using pre-packed silica gel or C-18 cartridges (RediSep). All final compounds were purified to >95% purity, as determined by a HPLC Breeze from Waters Co. using an Atlantis T3 5.0 μM 4.6 mm

×150 mm reverse phase column. 1D and 2D NMR spectra were recorded on a Bruker 600 MHz instruments. Chemical shifts are reported in ppm (δ) relative to ^{1}H (Me_4Si at 0.00 ppm), coupling constant (*J*) are reported in Hz throughout, and NMR signal assignments were based on DEPT, 2D [^{13}C, ^{1}H]-HSQC, 2D [^{1}H, ^{1}H]-COSY, 2D [^{1}H, ^{1}H]-TOCSY, and 2D [^{1}H, ^{1}H]-HMBC experiments. Low resolution and high-resolution mass spectral data were acquired on an Esquire LC00066 Mass Spectrometer, an Agilent ESI-TOF Mass Spectrometer, or a Bruker Daltonic Autoflex Maldi-Tof/Tof Mass Spectrometer. Detailed synthetic procedures and analytical data for compound intermediates and final compounds are reported in the Supplementary Material section.

Protein expression and purification

–The DNA sequence (Codons are optimized for *E. coli*) encoding for the EphA2 receptor (GENE ID: 1969 EPHA2) ligand binding domain (residues 27-200) was synthesized by GenScript USA Inc. (Piscataway, NJ 08854, USA) and subcloned into pET15b using the NdeI and BamHI cloning sites. In order to increase the protein solubility, 10 glutamic acids were added to the C-terminus. The resulting protein contains the EphA2 ligand binding domain (residues 27-200) with 21 extra amino acid residues (MGSSHHHHHHSSGLVPRGSHM) at the N-terminus and 10 glutamic acids at the C-terminus added to increased solubility. The protein was expressed in the Rosetta-gami B(DE3) pLysS competent cells with 0.5 mM IPTG at 20° C and purified using Ni^{2+}affinity chromatography. Uniformly ^{15}N-labeled protein was produced by growing the expression strain in M9 medium with $^{15}NH_4Cl$ as the sole nitrogen source.

Protein-ligand interaction

– NMR spectra were acquired on a 600 MHz Bruker Avance spectrometer equipped with a TCI-cryoprobe. ITC were measured with Model ITC200 from Microcal/GE Life Sciences.

ELISA-based competition and binding assays

– For competition assays, EphA2 Fc (R&D Systems, Minneapolis, MN) diluted to 1 μg/mL in TBST buffer (150 mM NaCl, 50 mM Tris-HCl, pH 7.5, with 0.01% Tween 20) was immobilized in protein A coated wells. The wells were then incubated for 3 h with 40 μl 0.01 nM ephrin-A5 fused to alkaline phosphatase (ephrin-A5 AP) in culture medium diluted in TBST in the presence of different concentrations of YNH-PTX or dYNH-PTX. The concentration of ephrin-A5 AP was calculated based on AP activity measurements. Bound ephrin-A5 AP was quantified by adding pNPP as the substrate and measuring the absorbance at 405 nm. Absorbance from wells where human Fc (R&D Systems, Minneapolis, MN) was immobilized instead of EphA2 Fc was subtracted as the background. Curves for EphA2 Fc binding to YSA-PTX, YNH-PTX, dYNH-PTX and DYP-PTX were determined by adding different concentrations of EphA2 Fc to high binding capacity ELISA half-well plates (Corning, Corning, NY, USA) precoated with streptavidin (Pierce Biotechnology, Rockford, IL) and 20 μl 1 μM biotinylated peptides. Bound EphA2 Fc was detected with an AP conjugated anti-human IgG antibody (Promega, San Luis Obispo, CA, 1:2,000 dilution in TBST). Absorbance at 405 nm was measured following incubation with 0.2 m g/m L 2, 2′-azino-bis(3-ethylbenzthiazoline-6-sulfonic acid) (ABTS) (Sigma-Aldrich, Steinheim, Germany) in citric acid as a substrate, and the absorbance in wells without EphA2 was subtracted as background. Inhibition and binding curves were analyzed using nonlinear regression and the program Prism (GraphPad Software Inc.).

Fluorescence cell imaging

– PC-3M-luc-C6 Bioware® (Caliper) and LNCaP prostate cancer cells (ATCC) were grown in RPMI 1640 medium (Mediatech, Inc, Herndon, VA) with 10% FBS and Pen/Strep. For

quantum dot internalization experiments, PC3M and LNCaP cells were grown overnight on glass coverslips. The conditioned medium was then removed from the cells, supplemented with 10 mM HEPES and stored at 4 °C, and the cells were serum starved for 3 hours in serum-free medium. The cells were then treated with 300 μl of 100 μM biotinylated YNH-PTX, dYNH-PTX, YSA-PTX or DYP-PTX in quantum dot-binding buffer for 20 min on ice, followed by 20 nM streptavidin-conjugated Qdot 655 (Invitrogen/Molecular Probes, Eugene, OR) in binding buffer for 20 min on ice. After removing the quantum dot solution, the cells were washed with the binding buffer and incubated with the stored conditioned medium in a 37°C CO_2 incubator for 2 hours to allow internalization of the EphA2-peptide-PTX-quantum dots complexes. The cells were then washed with ice cold PBS, fixed in 4% formaldehyde for 10 min, permeabilized for 3 min with 0.5% Triton-X100 in PBS, and incubated for 1 hour with PBS containing 10% goat serum. For EphA2 staining, the coverslips were incubated with a rabbit anti-EphA2 antibody (Life Technologies/Invitrogen) followed by a secondary anti-rabbit antibody conjugated with Alexa Fluor 488 (Life Technologies/Molecular Probes). For staining of lysosomes, the coverslips were incubated with polyclonal rabbit anti-human Lamp1 antibody (44) followed by a secondary anti-rabbit antibody conjugated with Alexa Fluor 568 (Life Technologies/Molecular Probes). The nuclei were counterstained with DAPI. Images were obtained with an Inverted TE300 Nikon fluorescence microscope and processed using Adobe Photoshop.

To image EphA2 internalization and co-localization with lysosomes after stimulation with ephrin-A1 Fc or the PTX-coupled peptides, PC3M cells plated on glass coverslips were serum starved for 1 hour in serum-free medium and then stimulated with 0.2 μg/mL Fc (as a negative control), 0.2 μg/mL ephrin-A1 Fc (as a positive control), or 100 μM PTX-coupled peptides for 2 hours. The cells were then fixed, permeabilized and labeled as described above. Images were acquired using a Radiance 2100 MP confocal microscope.

Immunoprecipitation and immunoblotting

– PC-3M-luc-C6 cells were serum-starved for 1 hour in serum-free medium and treated for 1 hour with 0.2 μg/mL human Fc (as a negative control), 0.2 μg/mL ephrin-A1 Fc (as a positive control), 100 μM YSA-PTX, 100 μM DYP-PTX, 100 μM YNH-PTX, or 100 μM dYNH-PTX. The cells were then placed on ice, rinsed once with cold PBS and incubated for 20 min at 4°C with a 0.5 mg/mL EZ-link sulfo-NHS-biotin (Thermo Scientific/Pierce, Rockford, IL) in PBS. The cells were then washed 3 times with a 100 mM glycine in PBS to quench the biotinylation reaction, followed by PBS. The cells were lysed in modified RIPA lysis buffer (150 mM NaCl, 1 mM EDTA, 1% Triton X-100, 1% sodium deoxycholate, 0.1% SDS, 20 mM Tris, pH 8.0) containing protease inhibitors and 1 mM sodium orthovanadate. For immunoprecipitations, the lysates were incubated with 1 μg anti-EphA2 antibody (Millipore-Upstate, Inc. Temecula, CA) immobilized on GammaBind Sepharose beads (GE Healthcare Life Sciences). Immunoprecipitates and lysates were probed by immunoblotting with an anti-phosphotyrosine antibody (Millipore, Inc, Temecula, CA), streptavidin coupled to HRP (Thermo Scientific/Pierce, Rockford, IL), or anti-EphA2 ant i b o d y (Life Technologies/Invitrogen). Lysates of PC-3M-luc-C6 and RENCA cells were probed by immunoblotting with the EphA2 Millipore antibody and with a GAPDH antibody (AbCam).

Measurement of peptide stability

– The peptides were incubated at 37°C with cultured PC3 cells or in mouse serum for different times. Medium diluted 1:3 or serum diluted 1:20 (corresponding to a final concentration of 25 μM for YSA-PTX and YNH-PTX and 75 μM for dYNH-PTX) were incubated in ELISA wells pre-coated with protein A and EphA2 Fc for 2 hours in the presence of 40 μl 0.01 nM ephrin-A5 AP. Inhibition of EphA2-ephrin-A5 binding was

measured as described above. Absorbance from wells coated with Fc and incubated with ephrin-A5 AP and culture medium or serum was subtracted as the background. Absorbance obtained from wells incubated with culture medium or mouse serum not containing any peptide was used to determine the 0% inhibition level (0% peptide remaining) and absorbance obtained in the presence of the peptides mixed with culture medium or serum immediately before adding them to the ELISA wells was used for normalization (100% peptide remaining).

In vivo prostate cancer xenograft studies

– As general procedure, PC-3M-luc-C6 cells (1×10^6) were injected subcutaneously into 6-8 week old female athymic nude mice (Harlan Labs, CA) and the peptide-PTX conjugates were dissolved in a mixture of 84% PBS, 8% DMSO, and 8% water and injected in a 100 μL final volume.

For the experiment reported in Figure 6A, once the tumors reached palpable sizes averaging approximately 100 mm^3 per group, the mice were treated three times a week for three weeks with intravenous doses of vehicle (n = 4), PTX (5 mg/Kg; n = 4), or dYNH-PTX (15.3 mg/kg, hence a dose that is equimolar to the taxol dose; n = 5). Tumor sizes during treatment were measured using calipers. One mouse in the vehicle group and one mouse in the PTX group died at the beginning of the experiment and therefore were not included in the analysis. In the experiment reported in Figure 6B, once the tumors reached palpable sizes, the mice were treated three times a week for three weeks with intravenous doses of vehicle (n = 5), PTX (5 mg/Kg; n = 5), dYNH-PTX (15.3 mg/Kg; n = 5), DYP-PTX (15.9 mg/Kg; n = 5), YSA-PTX (15.9 mg/Kg; n = 5). The dose of peptide-drug conjugates was equimolar to the taxol dose. Tumors in the dYNH-PTX-treated group became undetectable after 14 days of treatment. Hence, statistical analysis for this group could not be performed.

The experiment reported in supplementary Figure S1 was similarly carried out. Once the tumors reached palpable sizes averaging approximately 230 mm^3 per group, the mice were treated three times a week for three weeks with intravenous doses of vehicle (n = 8), PTX (10 mg/Kg; n = 8), DYP-PTX (31.8 mg/Kg; n = 8), and YSA-PTX (31.8 mg/Kg; n = 7). All doses of peptide-drug conjugates were equimolar to the taxol dose. Tumor sizes during treatment were measured using calipers. In the YSA-PTX treated group, one mouse died at the beginning of the experiment and therefore was not included in the analysis.

In vivo renal cancer allograft studies

– RENCA cells (1×10^6) were harvested from non-confluent monolayer cell cultures and mixed with 30 μL of rat-tail collagen. The cells were grafted under both renal capsules of BALB/c mice (Harlan Labs, CA) as previously described (45, 46). Three weeks following grafting, the mice were injected every 2 days with intravenous doses of vehicle (n = 4 mice), PTX (20 mg/kg; n = 4 mice), or dYNH-PTX (at a dose that is approximately equimolar to the taxol dose, 60 mg/kg; n = 5 mice) for a total of three injections. Both dYNH-PTX and PTX were dissolved in a mixture of 84% PBS, 8% DMSO and 8% Tween and injected in a 100 μl final volume. After one-week treatment, the mice were sacrificed. The grafts were then harvested, tumor volume calculated, and photographed. Endothelial cells were visualized by immunohistochemistry with anti-CD31 antibody (1:50, Abcam) using paraformaldehyde fixed, paraffin embedded 5 μm tissue sections. CD31-positive vascular outlines were measured from at least five 10 × images per tumor (n ≥ 8 tumors/group) using Image J software (NIH).

Supplementary Material

Refer to Web version on PubMed Central for supplementary material.

Acknowledgments

Financial support was obtained in part by NIH grant CA138390 to MP and EBP, and from Kure-It to NAB. We thank Dr. Andrey Bobkov for assistance with ITC measurements.

REFERENCES

1. Wang S, Placzek WJ, Stebbins JL, Mitra S, Noberini R, Koolpe M, et al. Novel targeted system to deliver chemotherapeutic drugs to EphA2-expressing cancer cells. J Med Chem. 2012; 55:2427–36. [PubMed: 22329578]
2. Gangloff A, Hsueh WA, Kesner AL, Kiesewetter DO, Pio BS, Pegram MD, et al. Estimation of paclitaxel biodistribution and uptake in human-derived xenografts in vivo with (18)Ffluoropaclitaxel. Journal of nuclear medicine : official publication, Society of Nuclear Medicine. 2005; 46:1866–71.
3. Sugahara KN, Teesalu T, Karmali PP, Kotamraju VR, Agemy L, Greenwald DR, et al. Coadministration of a tumor-penetrating peptide enhances the efficacy of cancer drugs. Science. 2010; 328:1031–5. [PubMed: 20378772]
4. Wu P, Malkoch M, Hunt JN, Vestberg R, Kaltgrad E, Finn MG, et al. Multivalent, bifunctional dendrimers prepared by click chemistry. Chemical communications. 2005:5775–7. [PubMed: 16307142]
5. Jaracz S, Chen J, Kuznetsova LV, Ojima I. Recent advances in tumor-targeting anticancer drug conjugates. Bioorg Med Chem. 2005; 13:5043–54. [PubMed: 15955702]
6. Langer R. New methods of drug delivery. Science. 1990; 249:1527–33. [PubMed: 2218494]
7. Schrama D, Reisfeld RA, Becker JC. Antibody targeted drugs as cancer therapeutics. Nat Rev Drug Discov. 2006; 5:147–59. [PubMed: 16424916]
8. van Vlerken LE, Amiji MM. Multi-functional polymeric nanoparticles for tumour-targeted drug delivery. Expert Opin Drug Deliv. 2006; 3:205–16. [PubMed: 16506948]
9. Leader B, Baca QJ, Golan DE. Protein therapeutics: a summary and pharmacological classification. Nat Rev Drug Discov. 2008; 7:21–39. [PubMed: 18097458]
10. Marx JL. Monoclonal antibodies in cancer. Science. 1982; 216:283–5. [PubMed: 7063886]
11. Aina OH, Liu R, Sutcliffe JL, Marik J, Pan CX, Lam KS. From combinatorial chemistry to cancer-targeting peptides. Mol Pharm. 2007; 4:631–51. [PubMed: 17880166]
12. Brown KC. Peptidic tumor targeting agents: the road from phage display peptide selections to clinical applications. Current pharmaceutical design. 2010; 16:1040–54. [PubMed: 20030617]
13. Corti A, Curnis F. Tumor vasculature targeting through NGR peptide-based drug delivery systems. Current pharmaceutical biotechnology. 2011; 12:1128–34. [PubMed: 21470145]
14. Cutrera J, Dibra D, Xia X, Hasan A, Reed S, Li S. Discovery of a linear peptide for improving tumor targeting of gene products and treatment of distal tumors by IL-12 gene therapy. Molecular therapy : the journal of the American Society of Gene Therapy. 2011; 19:1468–77. [PubMed: 21386825]
15. Hatakeyama S, Sugihara K, Shibata TK, Nakayama J, Akama TO, Tamura N, et al. Targeted drug delivery to tumor vasculature by a carbohydrate mimetic peptide. Proceedings of the National Academy of Sciences of the United States of America. 2011; 108:19587–92. [PubMed: 22114188]
16. Koivunen E, Arap W, Valtanen H, Rainisalo A, Medina OP, Heikkila P, et al. Tumor targeting with a selective gelatinase inhibitor. Nature biotechnology. 1999; 17:768–74.
17. Koolpe M, Dail M, Pasquale EB. An ephrin mimetic peptide that selectively targets the EphA2 receptor. J Biol Chem. 2002; 277:46974–9. [PubMed: 12351647]
18. Laakkonen P, Porkka K, Hoffman JA, Ruoslahti E. A tumor-homing peptide with a targeting specificity related to lymphatic vessels. Nature medicine. 2002; 8:751–5.

19. Newton JR, Deutscher SL. In vivo bacteriophage display for the discovery of novel peptidebased tumor-targeting agents. Methods in molecular biology. 2009; 504:275–90. [PubMed: 19159103]
20. Ruoslahti E. Targeting tumor vasculature with homing peptides from phage display. Seminars in cancer biology. 2000; 10:435–42. [PubMed: 11170865]
21. Wu HC, Chang DK. Peptide-mediated liposomal drug delivery system targeting tumor blood vessels in anticancer therapy. Journal of oncology. 2010; 2010:723798. [PubMed: 20454584]
22. Yang W, Luo D, Wang S, Wang R, Chen R, Liu Y, et al. TMTP1, a novel tumor-homing peptide specifically targeting metastasis. Clinical cancer research : an official journal of the American Association for Cancer Research. 2008; 14:5494–502. [PubMed: 18765541]
23. Lee TY, Wu HC, Tseng YL, Lin CT. A novel peptide specifically binding to nasopharyngeal carcinoma for targeted drug delivery. Cancer Res. 2004; 64:8002–8. [PubMed: 15520208]
24. Gersuk GM, Corey MJ, Corey E, Stray JE, Kawasaki GH, Vessella RL. High-affinity peptide ligands to prostate-specific antigen identified by polysome selection. Biochem Biophys Res Commun. 1997; 232:578–82. [PubMed: 9125226]
25. Ireton RC, Chen J. EphA2 receptor tyrosine kinase as a promising target for cancer therapeutics. Curr Cancer Drug Targets. 2005; 5:149–57. [PubMed: 15892616]
26. Pasquale EB. Eph receptors and ephrins in cancer: bidirectional signalling and beyond. Nat Rev Cancer. 2010; 10:165–80. [PubMed: 20179713]
27. Wykosky J, Debinski W. The EphA2 receptor and ephrinA1 ligand in solid tumors: function and therapeutic targeting. Mol Cancer Res. 2008; 6:1795–806. [PubMed: 19074825]
28. Kataoka H, Igarashi H, Kanamori M, Ihara M, Wang JD, Wang YJ, et al. Correlation of EPHA2 overexpression with high microvessel count in human primary colorectal cancer. Cancer Sci. 2004; 95:136–41. [PubMed: 14965363]
29. Ogawa K, Pasqualini R, Lindberg RA, Kain R, Freeman AL, Pasquale EB. The ephrin-A1 ligand and its receptor, EphA2, are expressed during tumor neovascularization. Oncogene. 2000; 19:6043–52. [PubMed: 11146556]
30. Landen CN, Kinch MS, Sood AK. EphA2 as a target for ovarian cancer therapy. Expert Opin Ther Targets. 2005; 9:1179–87. [PubMed: 16300469]
31. Noberini R, Lamberto I, Pasquale EB. Targeting Eph receptors with peptides and small molecules: Progress and challenges. Semin Cell Dev Biol. 2011
32. Tandon M, Vemula SV, Mittal SK. Emerging strategies for EphA2 receptor targeting for cancer therapeutics. Expert Opin Ther Targets. 2011; 15:31–51. [PubMed: 21142802]
33. Heroult M, Schaffner F, Augustin HG. Eph receptor and ephrin ligand-mediated interactions during angiogenesis and tumor progression. Exp Cell Res. 2006; 312:642–50. [PubMed: 16330025]
34. Mitra S, Duggineni S, Koolpe M, Zhu X, Huang Z, Pasquale EB. Structure-activity relationship analysis of peptides targeting the EphA2 receptor. Biochemistry. 2010; 49:6687–95. [PubMed: 20677833]
35. Scarberry KE, Dickerson EB, McDonald JF, Zhang ZJ. Magnetic nanoparticle-peptide conjugates for in vitro and in vivo targeting and extraction of cancer cells. J Am Chem Soc. 2008; 130:10258–62. [PubMed: 18611005]
36. Blackburn WH, Dickerson EB, Smith MH, McDonald JF, Lyon LA. Peptide-Functionalized Nanogels for Targeted siRNA Delivery. Bioconjug Chem. 2009; 20:960–8. [PubMed: 19341276]
37. Dickerson EB, Blackburn WH, Smith MH, Kapa LB, Lyon LA, McDonald JF. Chemosensitization of cancer cells by siRNA using targeted nanogel delivery. BMC Cancer. 2010; 10:10. [PubMed: 20064265]
38. Herrem CJ, Tatsumi T, Olson KS, Shirai K, Finke JH, Bukowski RM, et al. Expression of EphA2 is prognostic of disease-free interval and overall survival in surgically treated patients with renal cell carcinoma. Clin Cancer Res. 2005; 11:226–31. [PubMed: 15671550]
39. Coffman KT, Hu M, Carles-Kinch K, Tice D, Donacki N, Munyon K, et al. Differential EphA2 epitope display on normal versus malignant cells. Cancer Res. 2003; 63:7907–12. [PubMed: 14633720]
40. Macrae M, Neve RM, Rodriguez-Viciana P, Haqq C, Yeh J, Chen C, et al. A conditional feedback loop regulates Ras activity through EphA2. Cancer Cell. 2005; 8:111–8. [PubMed: 16098464]

41. Wakayama Y, Miura K, Sabe H, Mochizuki N. EphrinA1-EphA2 signal induces compaction and polarization of Madin-Darby canine kidney cells by inactivating ezrin through negative regulation of RhoA. J Biol Chem. 2011

42. Miura K, Nam JM, Kojima C, Mochizuki N, Sabe H. EphA2 engages Git1 to suppress Arf6 activity modulating epithelial cell-cell contacts. Mol Biol Cell. 2009; 20:1949–59. [PubMed: 19193766]

43. Liu Y, Zhang B, Yan B. Enabling anticancer therapeutics by nanoparticle carriers: the delivery of Paclitaxel. Int J Mol Sci. 2011; 12:4395–413. [PubMed: 21845085]

44. Carlsson SR, Roth J, Piller F, Fukuda M. Isolation and characterization of human lysosomal membrane glycoproteins, h-lamp-1 and h-lamp-2. Major sialoglycoproteins carrying polylactosaminoglycan. J Biol Chem. 1988; 263:18911–9. [PubMed: 3143719]

45. Li X, Placencio V, Iturregui JM, Uwamariya C, Sharif-Afshar AR, Koyama T, et al. Prostate tumor progression is mediated by a paracrine TGF-beta/Wnt3a signaling axis. Oncogene. 2008; 27:7118–30. [PubMed: 18724388]

46. Placencio VR, Sharif-Afshar AR, Li X, Huang H, Uwamariya C, Neilson EG, et al. Stromal transforming growth factor-beta signaling mediates prostatic response to androgen ablation by paracrine Wnt activity. Cancer Res. 2008; 68:4709–18. [PubMed: 18559517]

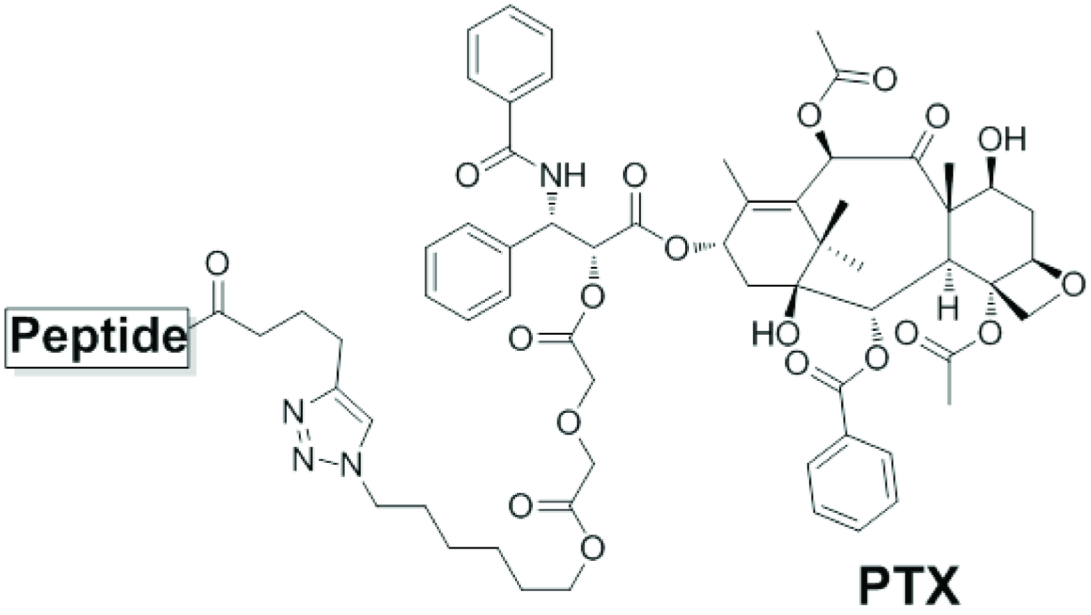

YNH-PTX Peptide = YSAYPDSVP(L-Norlecine)(L-Homoserine)S(K)
dYNH-PTX Peptide = ySAYPDSVP(L-Norlecine)(L-Homoserine)S(K)
DYP-PTX Peptide = DYPSMAMYSPSV(K)
YSA-PTX Peptide = YSAYPDSVPMMS(K)

Figure 1. Chemical structures of DYP, YSA, YNH, and dYNH peptide-drug conjugates
The terminal Lys residues is in parenthesis indicating that the amide bond between the residue and liker region takes place via its side chain amino group.

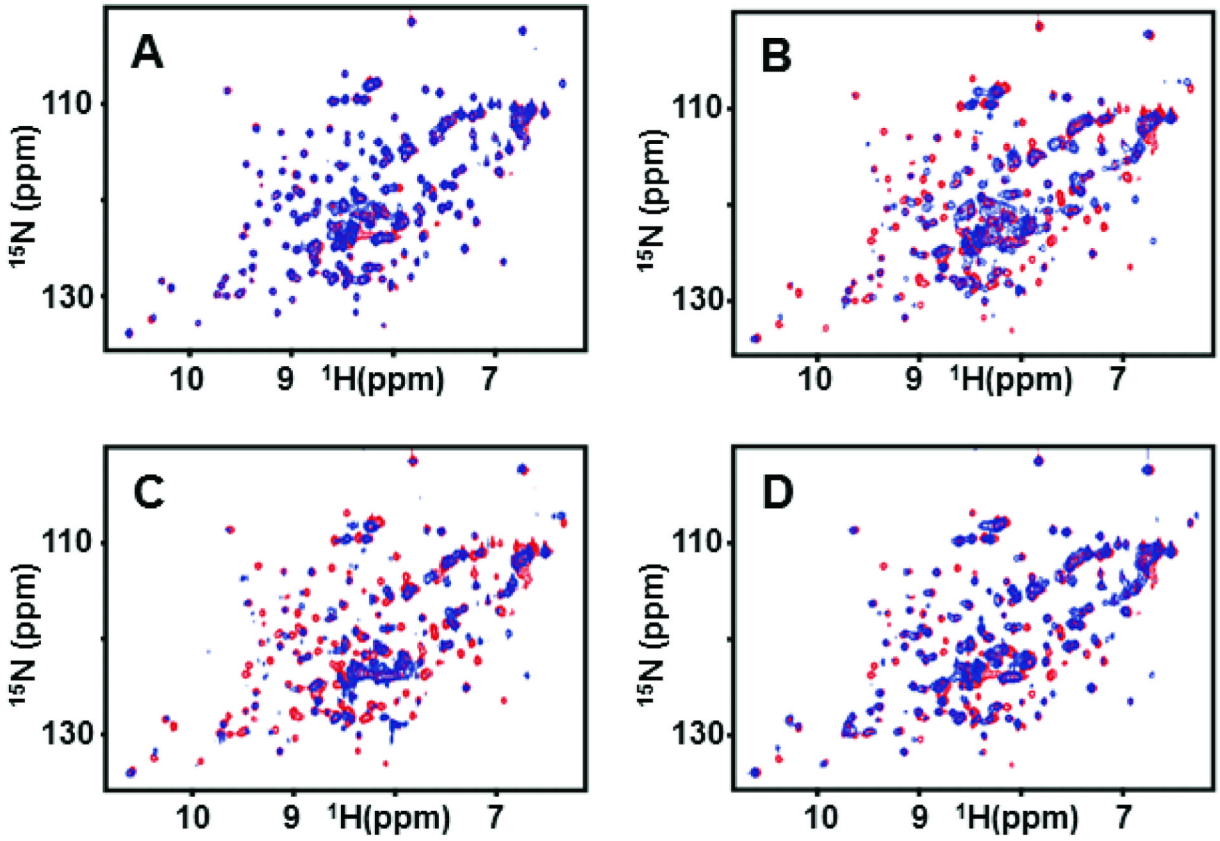

Figure 2. 2D NMR analysis of the binding of peptide-drug conjugates to EphA2

Superposition of 2D [^{15}N, ^{1}H]-HSQC spectra of 100 μM EphA2 in the absence (red) and presence (blue) of 200 μM DYP-PTX (A), YSA-PTX (B), YNH-PTX (C) and dYNH-PTX (D).

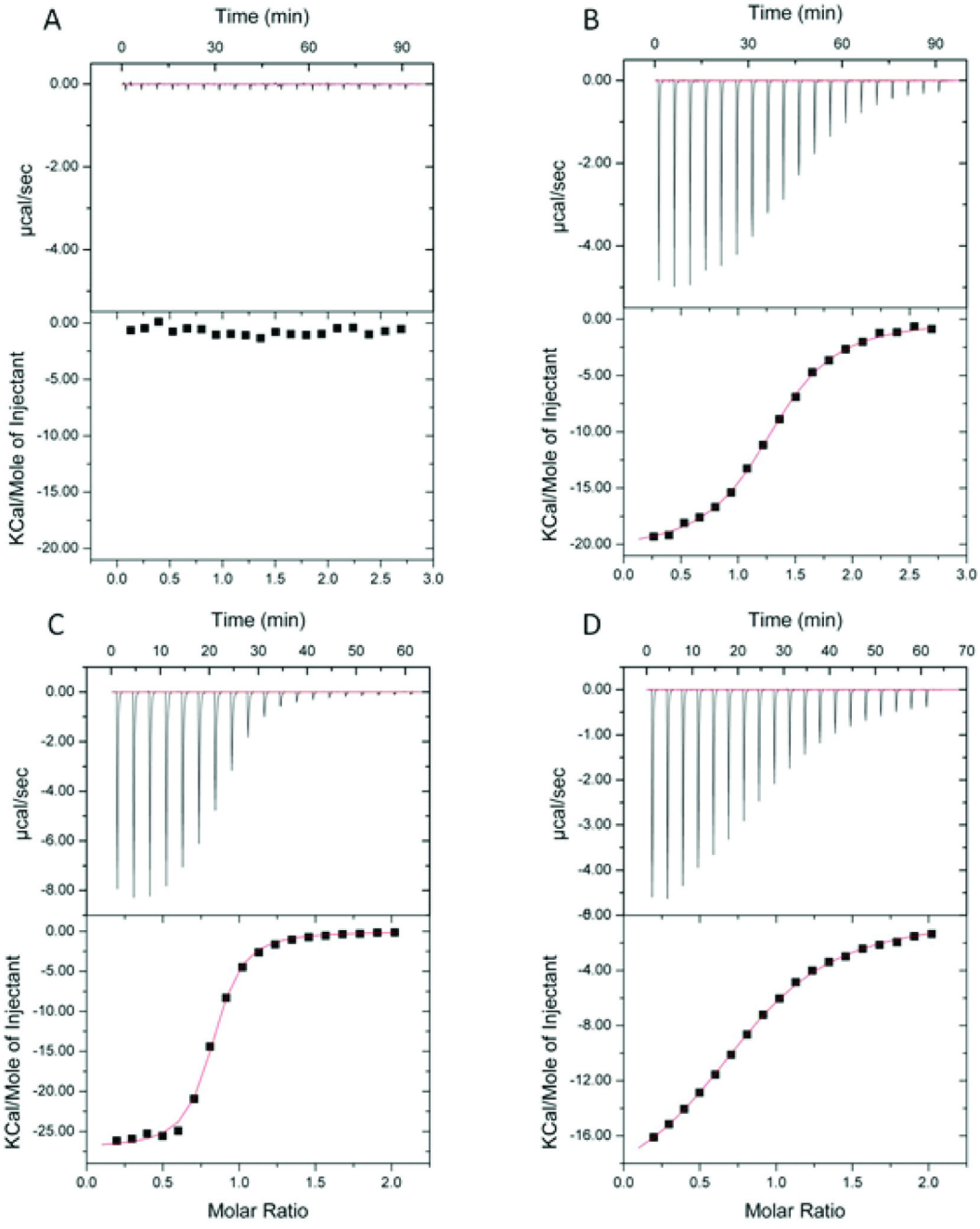

Figure 3. Binding affinities of the EphA2 targeting peptide-drug conjugates

Dissociation constants for the binding of the peptide-drug conjugates to the EphA2 ligand-binding domain (residues 27-200), as determined by isothermal titration calorimetry, are reported for (A) DYP-PTX, (B) YSA-PTX, (C) YNH-PTX and (D) dYNH-PTX.

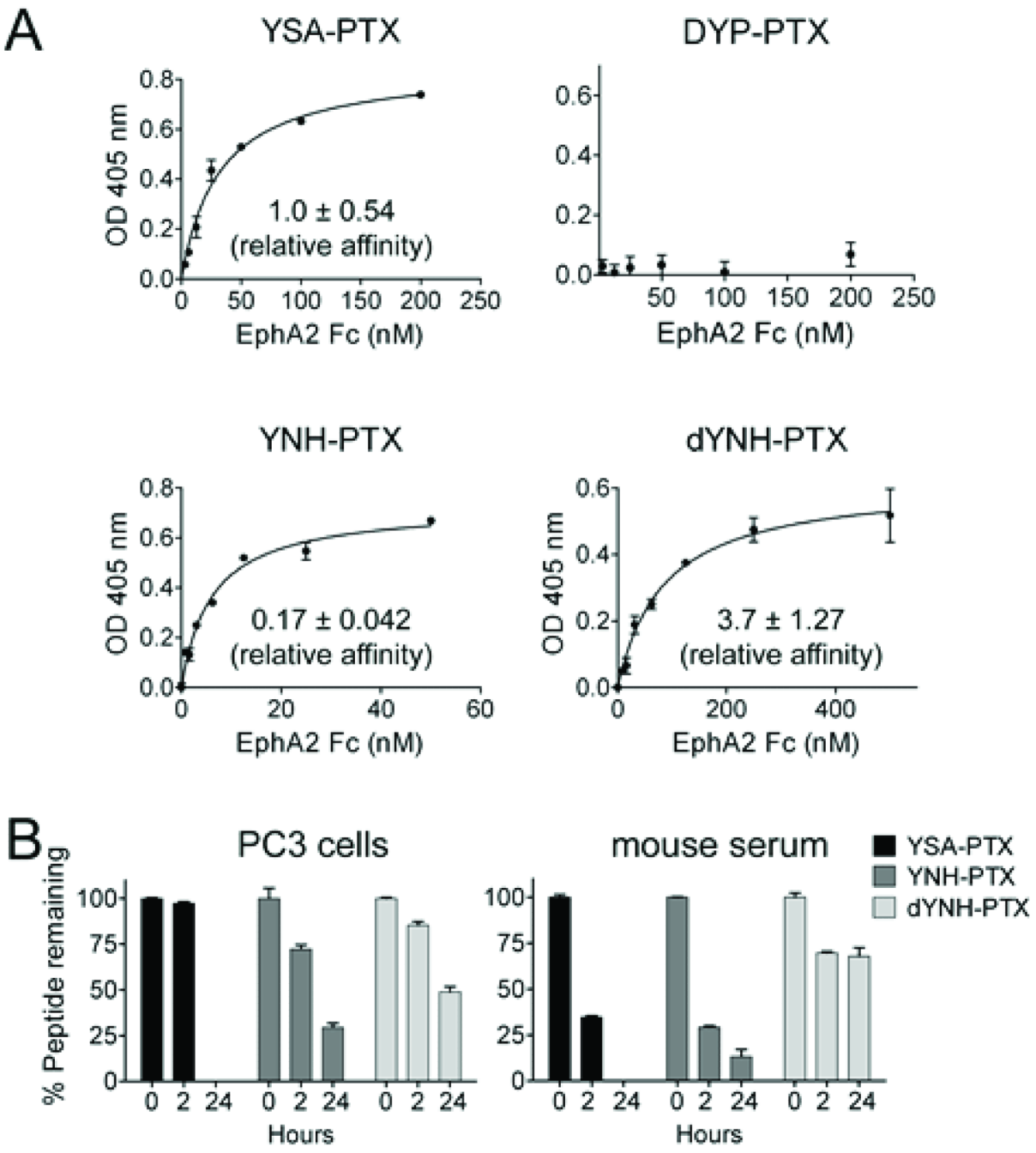

Figure 4. Affinity and stability of the EphA2 targeting peptide-drug conjugates

(A) Streptavidin-coated ELISA wells were incubated with biotinylated YSA-PTX, DYP-PTX, YNH-PTX or dYNH-PTX, followed by addition of EphA2 Fc at different concentrations. Bound EphA2 Fc was detected using an anti-human Fc antibody conjugated with AP. Apparent K_d values for the binding of the dimeric EphA2 Fc to the peptides were calculated and normalized to the values obtained for YSA-PTX (relative affinity = 1). The graphs show averages ± SE from triplicate measurements in representative experiments, while the relative affinity values are averages ± SE calculated from three experiments. (B) Peptide-drug conjugates were incubated with cultured PC3 cells or in mouse serum for the indicated times at 37°C and then tested for their ability to inhibit ephrin-A5 AP binding to

EphA2 Fc immobilized on ELISA wells. The concentrations of intact peptide-drug conjugates used (25 μM for YSA-PTX and YNH-PTX, 75 μM for dYNH-PTX) inhibit ephrin-A5 AP-EphA4 Fc binding by ~80-90%. The amount of peptide-drug conjugates remaining was estimated based on the ability to inhibit EphA2-ephrin-A5 interaction, with efficacy = 1 for the inhibition observed with the intact peptide-drug conjugates not incubated in culture medium or serum.

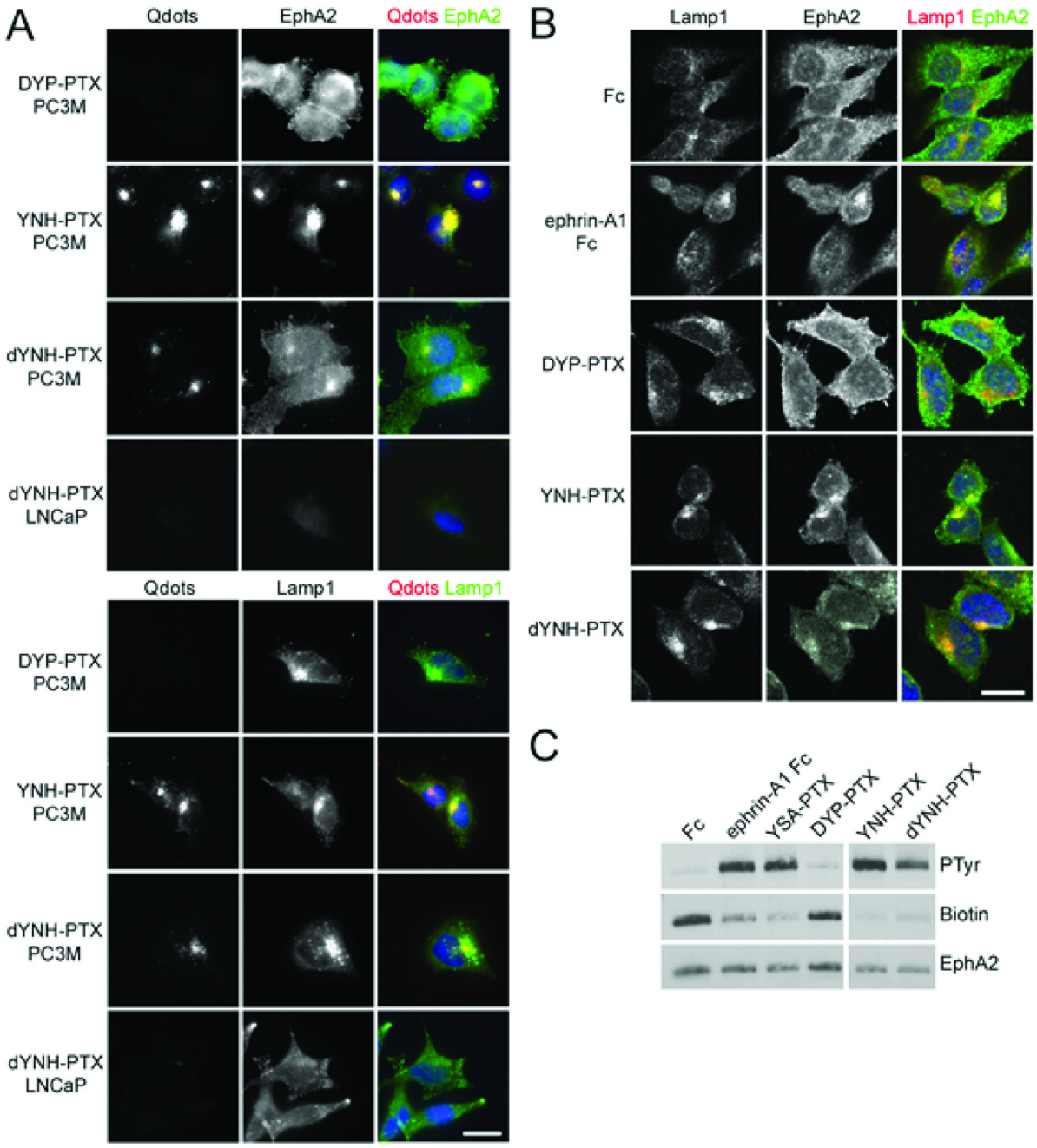

Figure 5. YNH-PTX and dYNH-PTX are internalized in cancer cells expressing EphA2

(A) PC3M or LNCaP prostate cancer cells were treated for 20 min with 100 μM YNH-PTX, dYNH-PTX or DYP-PTX, followed by a 20 min incubation with 20 nM streptavidin-conjugated red fluorescent Qdots. After removing the solution containing the peptides and the Qdots, the cells were incubated for 2 hrs at 37°C to allow receptor internalization. The cells were then stained for EphA2 (green, top panels) or the lysosomal marker Lamp1 (green, bottom panels) and DAPI (blue) to label nuclei. Scale bar = 25 μm. (B) PC3M cells were treated for 2 hours with 0.2 μg/mL ephrin-A1 Fc or 100 μM DYP-PTX, YNH-PTX or dYNH-PTX. The cells were stained for Lamp1 (red) and EphA2 (green) and nuclei were labelled with DAPI (blue). Representative confocal microscopy images are shown. Scale bar

= 25 μm. (C) PC3M cells were treated for 1 hour with 0.2 μg/mL ephrin-A1 Fc or 100 μM YSA-PTX, DYP-PTX, YNH-PTX or dYNH-PTX. Proteins present on the cell surface were then labeled with biotin. EphA2 immunoprecipitates were probed with an anti-phosphotyrosine antibody (PTyr), reprobed with streptavidin-HRP (biotin) and then with an anti-EphA2 antibody. All the lanes are from the same blot at the same exposure; irrelevant lanes between the DYP-PTX and YNH-PTX lanes were removed.

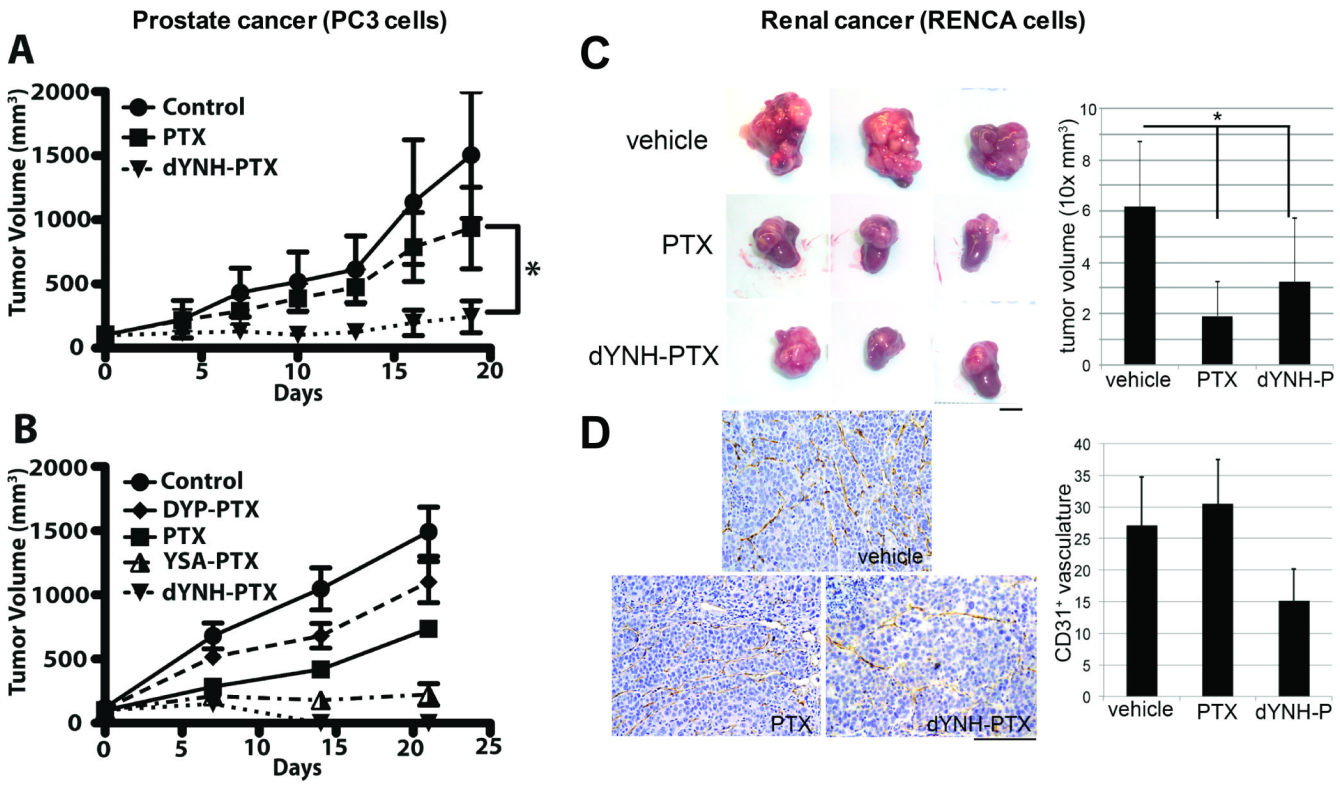

Figure 6. ***In vivo*** **effects of peptide-drug conjugates in two different tumor models**

(A) Groups of 4-5 athymic nude mice bearing pre-established subcutaneous PC3M tumors were treated three times weekly starting at day 0 with intravenous doses of vehicle (Control), PTX (5 mg/Kg) and dYNH-PTX (at a dose equimolar to the PTX dose). Tumor sizes were measured and averages ± SE are shown. $p < 0.05$ for the comparison of dYNH-PTX with PTX control, by repeated-measures two-way ANOVA. (B) Groups of 5 athymic nude mice bearing pre-established subcutaneous PC3M tumors were treated three times weekly starting at day 0 with intravenous doses of vehicle (Control), PTX (5 mg/Kg) and the indicated peptide-drug conjugates (at a dose equimolar to the PTX dose). Average tumor sizes ± SE are shown. (C) Groups of 4-5 BALB/c mice allografted with RENCA cells in the subrenal capsule were treated for one week with vehicle, PTX (5 mg/Kg) or dYNH-PTX (at a dose equimolar to the PTX dose) starting three weeks after tumor cell implantation. Tumor sizes were measured and averages ± SD are shown. The average volumes of tumors treated with PTX or dYNH-PTX were significantly different from the volume of tumors treated with vehicle ($p < 0.003$). Scale bar = 5 mm. (D) Immunohistochemical staining of the blood vessels in the tumor sections using an anti-CD31 antibody showed a significant decrease in the vasculature of the dYNH-PTX-treated tumors (labeled as dYNH-P) compared to either vehicle- or PTX-treated tumors (two-way ANOVA, $p = 0.001$). Scale bar = 5 μm.